

Structure Characterization and Mechanism of Growth of PbTe Nanocrystals Embedded in a Silicate Glass

A. F. Craievich,^{1,*} G. Kellermann,² L. C. Barbosa,³ and O. L. Alves⁴

¹*Institute of Physics, USP, São Paulo, SP, Brazil*

²*National Synchrotron Light Laboratory (LNLS), Campinas, SP, Brazil*

³*Institute of Physics, UNICAMP, Campinas, SP, Brazil*

⁴*Institute of Chemistry, UNICAMP, Campinas, SP, Brazil*
(Received 23 January 2002; published 15 November 2002)

A nanocomposite consisting of PbTe nanocrystals embedded in a silicate glass was studied by small-angle x-ray scattering during the early stage of isothermal annealing at 793 K. A theoretical function based on a model of spherical PbTe nanocrystals surrounded by a Pb and Te depleted shell fits well to all experimental curves. The time dependences of the nanocrystal radius and size of the depleted shell agree with the prediction of the theory of nucleation and growth by the classical mechanism of atomic diffusion.

DOI: 10.1103/PhysRevLett.89.235503

PACS numbers: 61.46.+w, 61.10.-i, 81.07.-b, 81.16.-c

Silicate glasses containing semiconductor PbTe nanocrystals exhibit nonlinear optical properties in the infrared [1] making them good candidates for telecommunication devices. A glass-PbTe nanocomposite tailored for practical application consists of isolated nanocrystals located farther away from the others. PbTe nanocrystals grown in a glass matrix are nearly spherical and exhibit a more or less narrow size distribution depending on the thermal history of the sample [2]. The glass matrix is structurally homogeneous and exhibits a very low absorption coefficient in the visible and near infrared.

The purpose of this investigation is to characterize the structure of PbTe nanocrystals embedded in a silicate glass matrix and establish the mechanism of the early stages of their formation and growth using small-angle x-ray scattering (SAXS) and complementary techniques. The optical properties of the studied nanocomposites depend on the size, shape, and composition profile of the nanocrystals. Therefore, the detailed knowledge of the local structure of the nanocrystals and their mechanism of growth is a basic requirement in order to explain the properties and verify the validity of related theoretical models [3].

The composition of the sample is 59SiO₂-15Na₂O-15ZnO-5Al₂O₃-2F-2PbO-2Te (wt %). The precursor raw substances were mixed and melted in a furnace at 1573 K. After 1 h at this temperature, the melt was poured between two metallic blocks that were then driven one against the other by a strong spring. This splat-cooling procedure yields thin (about 100- μ m-thick) glass samples. The as-quenched glass was first submitted to a crystal nucleation pre-annealing at 723 K during 19 h and then studied by *in situ* SAXS during isothermal annealing at 793 K. A specially designed high temperature cell was used to maintain the sample at a constant high temperature allowing for the diffusion of Pb and Te species through the glass matrix during *in situ* recording of successive SAXS curves.

The optical absorption coefficient of the studied material annealed during 30 min at $T = 793$ K was measured in order to detect the presence of PbTe semiconductor nanocrystals, determine the electron energy gap, and deduce from it an estimate of the nanocrystal average radius. The experimental spectrum, shown in Fig. 1, exhibits a sharp absorption reduction in the wavelength range $3000 \text{ \AA} < \lambda_o < 4000 \text{ \AA}$ (corresponding to an energy gap $E_g \approx 3.5$ eV). On the other hand, the energy gap for bulk PbTe crystals is known to be $E_g = 0.34$ eV, so corresponding an edge in the optical absorption at $\lambda_o \approx 36500 \text{ \AA}$. The strong “blueshift” in the optical absorption of the sample studied here is a consequence of electron quantum confinement effects associated with the existence of extremely small PbTe crystals embedded in the glass. A recent theoretical study of the electronic

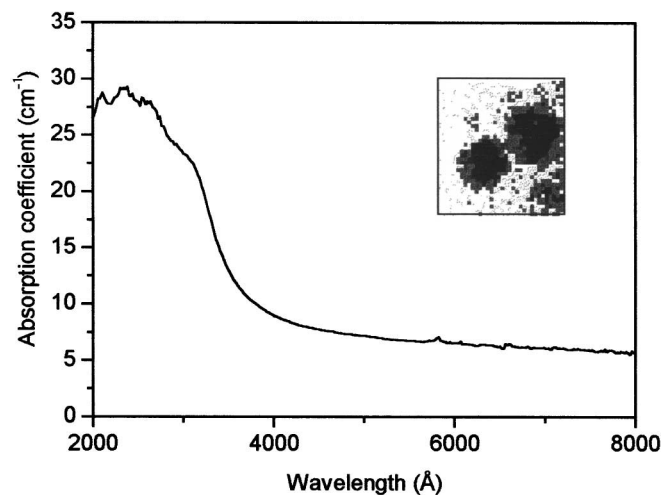


FIG. 1. Optical absorption spectrum of the PbTe-glass composite annealed 30 min at 793 K. Inset: TEM image showing two spherical PbTe nanocrystals with radii R equal to 40 and 50 \AA .

structure of several semiconductor nanocrystals [3] indicates that an energy gap of about 3.5 eV corresponds to spherical PbTe crystals with a radius $R \cong 14$ or 18 \AA depending on the band model. The observed spectroscopic properties are consistent with the model of formation and progressive growth of nanometric PbTe crystals proposed in the present study.

A preliminary transmission electron microscopy (TEM) analysis carried out at LME, National Synchrotron Light Laboratory (LNLS, Campinas, Brazil), indicated that the nanocrystals studied here are homogeneously distributed in the glass matrix and exhibit some size polydispersivity. The TEM image shown in the inset of Fig. 1 suggests that the nanocrystals are nearly spherical and exhibit a rather well-defined crystal-glass interface.

The SAXS measurements were performed at the synchrotron SAS beam line of LNLS. The SAXS intensity was determined as a function of the modulus of the scattering vector $q = (4\pi/\lambda)\sin\theta$, $\lambda = 1.609 \text{ \AA}$ being the x-ray wavelength and θ half of the scattering angle. The SAXS spectra $I(q)$ were recorded *in situ*, every 2 min. The experimental SAXS intensity produced by the studied Pb and Te doped glass sample corresponding to the shortest annealing time ($t = 2$ min) at 793 K is very weak and nearly q independent. This implies that the quenching procedure is actually efficient, avoiding a significant aggregation of Pb and Te atoms during sample cooling, and that the PbTe nuclei formed during the pre-annealing are very small. The scattering curve corresponding to $t = 4$ min exhibits an incipient peak located at $q \cong 0.09 \text{ \AA}^{-1}$. This off-zero peak progressively becomes more pronounced and shifts down to $q \cong 0.06 \text{ \AA}^{-1}$ for $t = 30$ min.

For a *concentrated* set of particles, a pronounced maximum in SAXS intensity curves at $q \neq 0$ is expected as a consequence of interparticle interference effects [4]. However, for a *dilute* system such as that studied here, the existence of significant interparticle interference effects can safely be disregarded. On the other hand, since the maximum of the SAXS curves progressively shifts toward low q from the very beginning of the process and no crossover of the different scattering curves is apparent, spinodal decomposition can be ruled out. The SAXS peak at $q \neq 0$ may alternatively be explained by the existence of a dilute set of PbTe nanocrystals surrounded by Pb and Te depleted shells around them. This model was applied in the past to explain the observation of well-defined rings in the small-angle scattering intensity produced by Guinier-Preston zones in Al-Ag alloys [4] and more recently in a FeSiBCuNb alloy [5].

The formation and growth of PbTe nanocrystals surrounded by a well-defined diffusion zone are expected during the first stages of annealing, when the aggregation process is controlled by the mechanism of classical diffusion of isolated atoms initially dispersed in the matrix [6]. In our case, Pb and Te atoms progressively aggregate

and build up the PbTe nanocrystals, thus reducing the supersaturation of the glass matrix. During the first stages of aggregation, only the Pb and Te atoms located close to the growing crystals incorporate to them. Based on these arguments, the structure and mechanism of formation and growth of PbTe nanocrystals in the studied system was modeled by the electron density function $\rho(r)$ shown in Fig. 2. The initial pre-annealed nanocomposite is assumed to be composed of a dilute set of spherical PbTe crystal nuclei with a constant electron density ρ_c embedded in a homogeneous glass matrix with a constant electron density ρ_0 [Fig. 2(a)]. During annealing, Pb and Te atoms diffuse from the glass to the nanocrystals, with growing radius $R(t)$, and form a depleted shell with spherical symmetry and an assumed Gaussian profile $[\rho(r) - \rho_0] \propto \exp(-3r^2/2R_g^2)$, where R_g is the radius of gyration associated to the 3D depleted shell [Fig. 2(b)]. We have considered as a first approximation that all growing nanocrystals and depleted shells have the same size.

The SAXS intensity produced by a dilute set of N similar and isotropic colloidal objects is N times the squared form factor of the object [4]. In our case, the form factor is that associated to a spherical PbTe nanocrystal surrounded by a depleted shell whose electron density is assumed to be described by a Gaussian function (Fig. 2). If $n(t)$ is the number of electrons corresponding to Pb and Te atomic species that migrated from the glass into the nanocrystal volume, coming from the depleted zone surrounding them, a good approximation for the function that describes the time dependent scattering intensity $I(q, t)$ is given by

$$I(q, t) = N(t)n(t)^2 \times \left\{ [1 + a(t)] \frac{3\{\sin[qR(t)] - qR(t)\cos[qR(t)]\}}{[qR(t)]^3} - e^{-[R_g(t)^2q^2]/6} \right\}^2, \quad (1)$$

where $a(t) = n_0/n(t)$, n_0 being the excess in electron number in the preexisting nuclei. Nonzero values of the function $a(t)$ indicate the presence of small nanocrystal nuclei at $t = 0$. Equation (1) has a maximum for $q \neq 0$ except for $t = 0$. If a dilute set of spherical particles exhibits a radius dispersion described by a normalized function $G(R)$, the SAXS intensity is simply given by $I_G(q) = \int I(q, R)G(R)dR$.

The experimental SAXS intensity curves of the studied nanocomposite, for different periods of isothermal annealing at 793 K, are plotted in Fig. 3(a) (symbols) together with the functions defined by Eq. (1) that best fit to the experimental results (continuous lines). For two-phase systems consisting of colloidal particles embedded in a homogeneous matrix and growing by the mechanism of coarsening, i.e., larger particles with equilibrium composition growing at the expense of the small ones, the integral of the scattering intensity in the reciprocal space

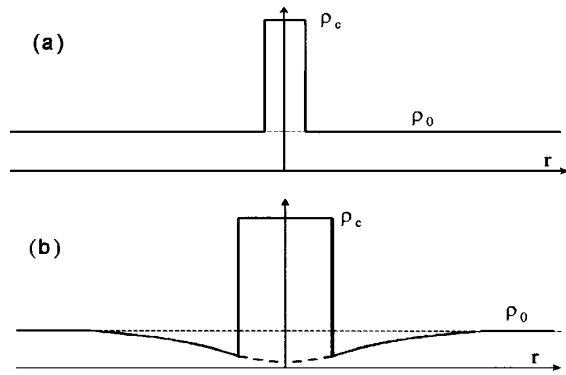


FIG. 2. Schematic model of the electron density function $\rho(r)$ corresponding to (a) a nanocrystal nucleus in an as-quenched and pre-annealed glass, before isothermal annealing, and (b) a nanocrystal surrounded by a depleted shell formed after isothermal annealing.

$Q = 4\pi \int I(q)q^2 dq$ is essentially a time invariant proportional to the total volume of the precipitate phase [4]. The integral of our experimental SAXS curves was determined and plotted as a function of the annealing time in Fig. 4. The clearly increasing trend of $Q(t)$ along the whole process rules out a pure mechanism of nanocrystal coarsening and provides additional support to the proposed classical mechanism of growth promoted by the diffusion of Pb and Te atoms toward growing PbTe nanocrystals that become surrounded by also growing depleted shells.

From the results of the fitting procedure illustrated in Fig. 3(a), the values of the parameters N , R , and R_g were determined as functions of the annealing time. We note that the $N(t)$ function, plotted in Fig. 4, exhibits a sharp increase during the very early stages of isothermal annealing and becomes approximately constant from $t \approx 7$ min until the end of the isothermal annealing. This indicates that all the nanocrystal nuclei are formed during the pre-annealing process and during the first few minutes of isothermal annealing.

The time variation of the radius of the PbTe nanocrystals predicted by the classical theory of isothermal growth of a single sphere embedded in an infinite and initially homogeneous matrix is given by $R(t) = (R_0^2 + kt)^{1/2}$ [7], where R_0 is the radius of the preexisting PbTe crystal nuclei at an annealing time $t = 0$, and k is a constant. This theoretical dependence in R versus t plots is actually observed (continuous line in Fig. 5) except during the first minutes of annealing ($t < 7$ min). A similar time dependence is apparent in Fig. 5 for the parameter R_g characterizing the overall size of the depleted shell.

Because of the inherent low resolution of SAXS analysis and the short counting times required for this *in situ* study, the excellent fittings of the functions defined by Eq. (1) to the experimental SAXS curves plotted in Fig. 3(a) provide only a qualitative support to the proposed structural model. In order to get better insight about the sharpness of the crystal-glass interface, a

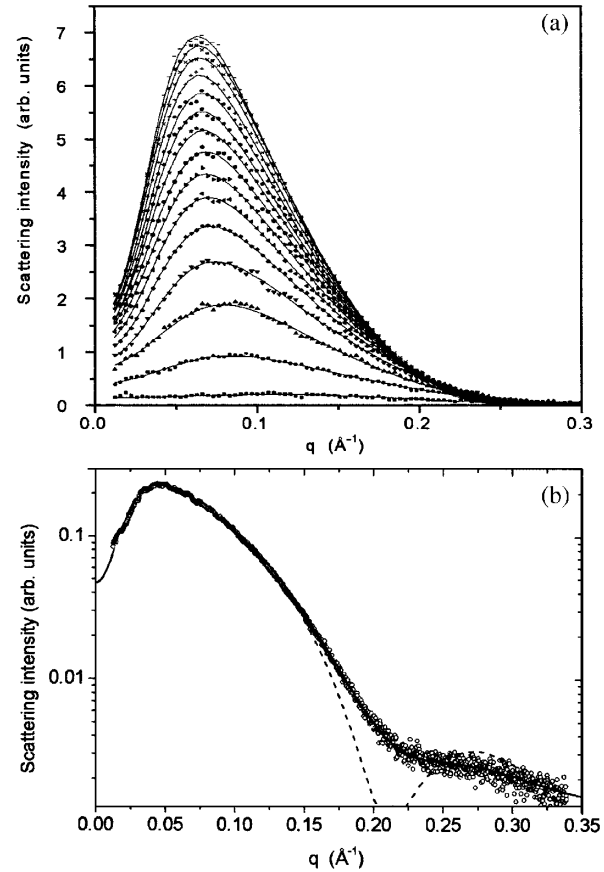


FIG. 3. (a) Symbols: Experimental SAXS curves determined *in situ* during isothermal annealing at 793 K. The annealing times associated with the scattering curves vary from $t = 2$ min (bottom) up to 30 min (top). Solid line: SAXS intensity functions defined by Eq. (1) that best fit to the experimental profiles. (b) Experimental SAXS curve (symbols) corresponding to a sample with a long *ex situ* annealing at 793 K. Dashed line: Function given by Eq. (1) that best fits to the experimental SAXS curve. Continuous line: Function determined assuming a Gaussian polydispersivity of crystal radii.

more precise analysis over the high q range of the SAXS curves is required. Figure 3(b) displays the scattering intensity, in logarithmic scale, produced by another sample of the same material with an equivalent composition and subjected to a longer *ex situ* annealing at the same temperature. The function defined by Eq. (1) for monodisperse systems that best fits to the experimental function is shown as a dashed line in Fig. 3(b). A much better fitting at high q was obtained assuming the same model for nanocrystals and depleted shells but allowing for a radius dispersion defined by a simple Gaussian function $G(R)$ with an average radius $\langle R \rangle = 22.0 \text{ \AA}$ and a relative standard deviation $\sigma/\langle R \rangle = 0.18$. The results given in Fig. 3(b) provides a stronger support to our basic assumption about the spherical shape and about the sharpness of the nanocrystal-glass interface and yields a quantitative information about the nanocrystal size polydispersivity.

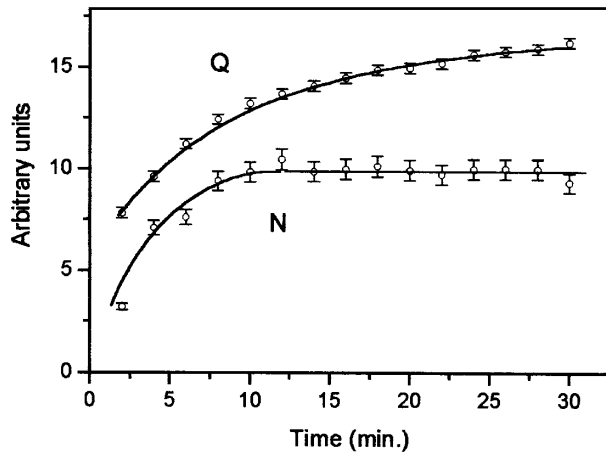


FIG. 4. Integral of the scattering intensity in reciprocal space (Q) and number of nanocrystals (N) as functions of the annealing time.

The deviations of N , R , and R_g from the values expected from the theory for atomic diffusion [7] for very short annealing times observed in Fig. 5 suggest the presence of a transient process affecting the diffusion rate of Pb and Te atoms. A similar effect was observed in a previous study of nanophase separation in borate glasses [8]. In this case, the transient increase in growth rate during the first stages of the process was attributed to an enhancing effect on the atomic diffusion rate produced by residual stresses that may develop during the severe quenching process. The results plotted in Fig. 5 suggest that the same type of stresses also develop in the presently studied material, thus increasing the growth rate of PbTe nanocrystals in the very early stage of annealing. Once the stresses are relaxed, R and R_g vary according to the theoretical prediction [7].

The presented results demonstrate that the structure of the studied nanocomposite can be modeled by spherical PbTe nanocrystals with a sharp crystal-glass interface surrounded by smooth depleted shells embedded in a homogeneous glass matrix. We have also demonstrated that the growth of the preexisting PbTe nuclei is controlled by the classical mechanism of atomic diffusion of individual Pb and Te atoms and that, at very early stages of the process, a transient deviation occurs.

The proposed structural model of spherical and stoichiometric PbTe nanocrystals embedded in a silicate glass matrix is also consistent with the main features of the observed optical properties. As a matter of fact, the blueshift of the optical absorption edge observed in the experimental spectra agrees with that theoretically determined [3] for spherical PbTe nanocrystals with the same radius as that derived from SAXS results. In order to detect finer effects on the optical properties produced by small deviations from spherical shape and/or by the presence of depleted diffusion zones around the nanocrystals, further *in situ* and simultaneous determinations of SAXS and optical absorption spectra are required.

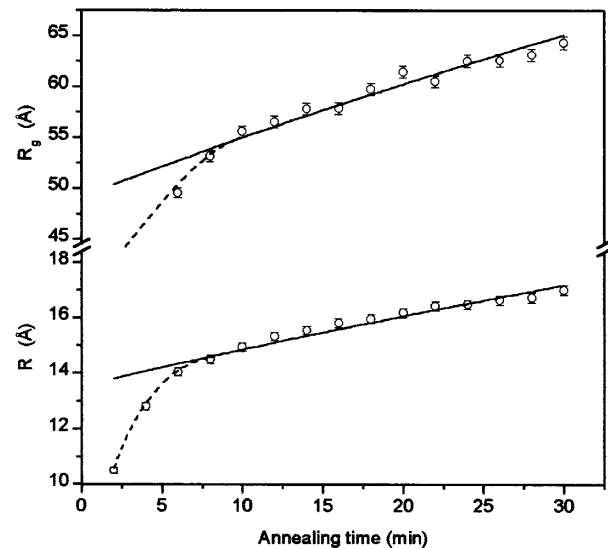


FIG. 5. Time variations of nanocrystal radius (R) and radius of gyration associated to the function describing the depleted shell (R_g).

A final comment concerns the observed clear difference between the shape of the SAXS curves plotted in Fig. 3(a), with a maximum at $q \neq 0$ for all time periods of annealing, and those corresponding to the previously studied PbTe nanocrystals embedded in a different borosilicate glass matrix annealed at 923 K [2] and to other similar nanocomposites that exhibit a maximum at $q = 0$. This different behavior indicates a difference in the predominant mechanism controlling the process of nanocrystal formation. In the case of the presently studied material, annealed at a rather low temperature ($T = 793$ K), the nanocrystal growth is controlled by a relatively slow atomic diffusion process of both Pb and Te species through the glass matrix leading to the formation of well-defined depleted shells around the crystals.

This work was supported by LNLS, PRONEX, and FAPESP.

*Permanent address: Institute of Physics, USP, CP 66318, CEP 05315-970, São Paulo-SP, Brazil.

Electronic address: craievich@if.usp.br

- [1] V. C. Reynoso *et al.*, *Electron. Lett.* **31**, 1013 (1995).
- [2] A. F. Craievich, O. L. Alves, and L. C. Barbosa, *J. Appl. Crystallogr.* **30**, 623 (1997).
- [3] G. E. Tudury *et al.*, *Phys. Rev. B* **62**, 7357 (2000).
- [4] A. Guinier, *X-ray Diffraction in Crystals, Imperfect Crystals and Amorphous Bodies* (Freeman, San Francisco, 1963).
- [5] A. Heinemann *et al.*, *J. Appl. Crystallogr.* **33**, 1386 (2000).
- [6] J. W. Christian, *The Theory of Transformations in Metals and Alloys* (Pergamon, New York, 1975).
- [7] J. Bartels *et al.*, *J. Non-Cryst. Solids* **136**, 181 (1991).
- [8] A. F. Craievich, *Phys. Status Solidi A* **28**, 609 (1975).